

# Wave-induced thermal flux and scattering of P waves in a medium with aligned circular cracks

Jia Wei<sup>1</sup>, Li-Yun Fu<sup>2</sup>, José M. Carcione<sup>3</sup>, and Tongcheng Han<sup>4</sup>

## ABSTRACT

High temperature affects the seismic properties of cracked and faulted reservoirs and can be an indicator for their detection. To this purpose, the authors study the wave-induced thermal flux (WITF) and develop two exact solutions for the scattering of compressional waves by a circular crack filled with a compressible fluid, in which the approach is based on thermally permeable and impermeable boundary conditions. The authors obtained the phase velocity and attenuation as a function of frequency, which found that there are two loss mechanisms, i.e., thermoelastic dissipation at low frequencies and elastic scattering at high frequencies. Basically, when the crack

size is comparable to the thermal and elastic wavelengths, there are substantial dispersion and attenuation (anelasticity) in the WITF and scattering frequency ranges, respectively. This means that the spatial inhomogeneity scale for inducing WITF is much smaller than that of scattering and the two mechanisms can be discriminated. The dependence of the compressional-wave velocity and attenuation on the compressibility and thermal expansion of the crack-filling fluid are different depending on the thermal diffusion rates at the crack interface. The anelasticity is much higher in the fully permeable case. This model has the potential to evaluate thermoelastic properties and heterogeneity at different scales from seismic responses.

## INTRODUCTION

Cracks of various sizes are widely observed in the lithosphere, which have a significant influence on the propagation of P and S waves (Carcione et al., 2020a). Scattering from these water-saturated cracks and from melted zones provides information about the earth structure and dynamics, in which temperature plays a key role (e.g., Romanowicz and Mitchell, 2007; Carcione et al., 2018b). Seismic scattering has been widely used for the detection of conventional hydrocarbon exploration because it is an indicator of the presence of cracks. However, the identification of tight oil and gas resources in unconventional resources such as source rocks, requires further research related to seismic scattering and attenuation (e.g., Fu, 2012, 2017). Aki (1980) states that thermoelasticity and elastic scattering are the two most viable models to describe seismic

attenuation at lithospheric temperatures, depending on the scale of the heterogeneities. However, it is not straightforward to decouple the effects of anelastic attenuation from scattering. Following Aki (1980), the purpose of our work is to study the combined effect of wave-induced thermal flux (WITF) and elastic scattering of P waves propagating in a thermoelastic medium with aligned circular cracks, with a particular focus on the separation of the two effects.

Thermoelasticity theory describes the relation between the fields of elastic deformation and temperature. Spatial stress variations during wave propagation in a cracked medium give rise to temperature fluctuations and hence to local thermal fluxes, which result in wave dissipation. This mechanism has been considered in geophysical studies (e.g., Zener, 1938; Treitel, 1959; Savage, 1966; Aki, 1980; Armstrong, 1984; Carcione et al., 2018c, 2019, 2020b), and the effects of temperature in geothermal prospecting (e.g.,

Manuscript received by the Editor 16 September 2021; revised manuscript received 30 January 2022; published online 1 July 2022.

<sup>1</sup>Chinese Academy of Sciences, Institute of Geology and Geophysics, Key Laboratory of Petroleum Resource Research, Beijing, China; University of Chinese Academy of Sciences, Beijing, China; and Chinese Academy of Sciences, Innovation Academy for Earth Science, Beijing, China. E-mail: jiawei@mail.iggcas.ac.cn.

<sup>2</sup>Qingdao National Laboratory for Marine Science and Technology, Laboratory for Marine Mineral Resources, Qingdao, China and China University of Petroleum (East China), Key Laboratory of Deep Oil and Gas, Qingdao, China. E-mail: lfu@upc.edu.cn (corresponding author).

<sup>3</sup>National Institute of Oceanography and Applied Geophysics (OGS), Trieste, Italy. E-mail: jcarcione@inogs.it.

<sup>4</sup>China University of Petroleum (East China), Key Laboratory of Deep Oil and Gas, Qingdao, China. E-mail: hantc@upc.edu.cn.

© 2022 Society of Exploration Geophysicists. All rights reserved.

Jacquey et al., 2015) and global seismology (e.g., Boschi, 1973; Parmentier and Haxby, 1986; Ritsema et al., 2011). Zener (1938) describes the physics of thermoelastic attenuation, and Biot (1956) proposes the differential equations of thermoelasticity based on the Fourier heat conduction law. However, this equation is parabolic, predicting discontinuities, and infinite velocities as a function of frequency contrary to actual observations. Savage (1966) investigates the thermoelastic attenuation of P and S waves for medium filled with spheres and cylindrical cavities or pores. Lord and Shulman (1967) modify the conventional Fourier law by introducing a relaxation term into the heat equation, which became hyperbolic and hence avoided those unphysical behaviors. Armstrong (1984) reports that the frequency dependence of thermal dissipation depends on the distribution and correlation of the heterogeneities. Carcinoid et al. (2020b) obtain analytical solutions of wave-induced thermoelastic attenuation in media with cavities or pores and thin periodic layers. Wei et al. (2020a) study the thermoelastic dispersion and attenuation of P- and SV-wave scattering by aligned cracks in an isothermal elastic medium. Numerical algorithms, based on the Lord-Shulman equations, were developed to compute synthetic seismograms in thermoelastic media (e.g., Carcione et al., 2018c; Hou et al., 2021), with Cercone et al. (2019) extending the simulations to the poroelasticity case. Moreover, Green's functions in the frequency domain were derived (Wang et al., 2020; Wei et al., 2020b). The results predict the presence of the classical P, and S waves and a thermal wave, which present diffusive behaviors under certain conditions and have characteristics similar to the slow P wave of poroelasticity.

In past decades, wave scattering in cracked media has been a subject of study for seismologists and rock physicists. Early works (e.g., Sezawa, 1927; Harumi, 1962; Martin, 1981) focused on the scattering by a single crack in an elastic solid. Then, the case of scattering by a set of randomly distributed aligned cracks was considered (e.g., Kikuchi, 1981; Yamashita, 1990; Zhang and Gross, 1993; Sato, 2021), based on the Floyd approximation (Foldy, 1945). These methods were further developed to study wave scattering by aligned fluid-saturated cracks in an elastic background medium (e.g., Kawahara and Yamashita, 1992; Guo et al., 2018c). On this basis, the Biot theory was used to investigate wave-induced fluid flow (WIFF) between the porous background and cracks (e.g., Galvin and Gurevich, 2009; Gurevich et al., 2009), in particular the effects on dispersion and attenuation of P waves (e.g., Brajanovski et al., 2005; Ba et al., 2016, 2017; Fu et al., 2018). Recently, an effective-medium model for S-wave dispersion and attenuation in porous media with spherical or cylindrical cracks was developed (Song et al., 2016a, 2016b). Many studies reveal that, when the crack size is comparable to the Biot slow P wavelength, there is significant dispersion and attenuation (e.g., Müller et al., 2010; Guo et al., 2018a, 2018b; Fu et al., 2020). The WIFF mechanism also can be described with an additional hydrodynamic equation (e.g., Chapman et al., 2002; Chapman, 2009; Shuai et al., 2020, 2022). However, most works assume that the crack-filling fluid is incompressible, thus only considering the WIFF effect and ignoring elastic scattering. More recently, Guo and Gurevich (2020) and Song et al. (2020) study the effects of coupling between WIFF and elastic scattering. Their results show that diffusion-type WIFF and elastic scattering dominate the anelasticity at low and high frequencies, respectively, but these models do not consider explicitly the temperature effects on wave propagation.

We investigate the coupling between WIFF and elastic scattering based on the Lord-Shulman equations of dynamic thermoelasticity. We first formulate the governing equations, and then derive the general solution and construct two pairs of dual integral equations under boundary conditions of fully thermal permeability and impermeability. These integrals are transformed to Fredholm integral equations of the second kind to obtain the exact solutions. Furthermore, the velocity dispersion and attenuation of P waves in a sparse distribution of aligned cracks are obtained by the Foldy approximation and the effect of the crack-filling fluid thermoelastic properties is analyzed, considering crack surfaces with different thermal diffusion.

## PROBLEM FORMULATION

We consider an incident harmonic plane P wave propagating in an infinite thermoelastic solid with aligned fluid-saturated cracks in the positive direction of the  $z$ -axis of a cylindrical polar coordinate system  $(r, \varphi, z)$ . A set of cracks with the same circular shape, radius  $a$ , and thickness  $d$  are sparsely, randomly, and homogeneously embedded in a thermoelastic nonporous background medium perpendicular to the  $z$ -axis (Figure 1a). To estimate the velocity dispersion and attenuation, the scattering of the incident P wave by a single circular crack should be studied first. We assume that the crack occupies the circle  $0 \leq r \leq a$  on the plane  $z = 0$  as shown in the oblique view (Figure 1b) and the front view (Figure 1c). The incident P wave can be expressed as  $u_z^{\text{in}} = u_0 e^{ik_p z}$ , where the superscript "in" denotes the incident field and  $u_0$  and  $k_p$  are the amplitude and wavenumber, respectively. The basic equations of dynamic thermoelasticity are formulated in this section, which provides the basis to study the coupling between WIFF and elastic scattering.

### Basic equations for dynamic thermoelasticity

We use the Lord-Shulman model to describe wave propagation in the thermoelastic background medium. The constitutive equations of thermoelasticity for the stress tensor  $\boldsymbol{\sigma}$  and the conservation of energy for the temperature disturbance  $\theta$  can be, respectively, expressed as (Biota; Carcione et al., 2020b; Wei et al., 2020a)

$$\begin{cases} \boldsymbol{\sigma} = \lambda \nabla \cdot \mathbf{u} + \mu (\nabla \mathbf{u} + \mathbf{u} \nabla) - \beta \theta \\ \theta = -\frac{T_0}{\rho c_E} \left( \beta \nabla \cdot \mathbf{u} - \frac{h}{T_0} \right) \end{cases}, \quad (1)$$

where  $\lambda$  and  $\mu$  are the Lamé constants of the background medium;  $\mathbf{u}$  is the displacement vector;  $T_0$  is the reference absolute temperature;  $\rho$  and  $c_E$  are the mass density and specific heat capacity of the thermoelastic medium, respectively;  $h$  is the amount of heat absorbed by the element; and  $\beta = (3\lambda + 2\mu)\alpha$  with  $\alpha$  being the coefficient of thermal expansion. Introducing the relation between the heat and thermal flux  $h = -\nabla \cdot \boldsymbol{\phi}$ , equation 1 becomes

$$\begin{cases} \boldsymbol{\sigma} = \lambda \nabla \cdot \mathbf{u} + \mu (\nabla \mathbf{u} + \mathbf{u} \nabla) - \beta \theta \\ \theta = -\frac{T_0}{\rho c_E} \left( \beta \nabla \cdot \mathbf{u} + \frac{\nabla \cdot \boldsymbol{\phi}}{T_0} \right) \end{cases}. \quad (2)$$

Furthermore, the dynamical equations in the Fourier domain are

$$\nabla \cdot \boldsymbol{\sigma} = -\omega^2 \rho \mathbf{u}, \quad (3)$$

where  $\omega$  is the angular frequency. The Lord-Shulman generalized equation of heat conduction

$$\nabla\theta = \omega^2 \hat{\rho} \frac{\phi}{T_0}, \quad \hat{\rho} = \frac{i T_0(1 - i\tau_0\omega)}{\omega \gamma}, \quad (4)$$

is required to avoid infinite velocities by introducing a relaxation term into the classical heat equation, where  $\tau_0$  and  $\gamma$  are the relaxation time and the coefficient of heat conduction, respectively. By substituting equation 2 into equations 3 and 4, we obtain the following governing equations of dynamic thermoelasticity:

$$\begin{cases} (H_{\text{tem}} - \mu)\nabla\nabla \cdot \mathbf{u} + \mu\nabla^2\mathbf{u} + \omega^2\rho\mathbf{u} + \beta\frac{T_0}{\rho c_E}\frac{\nabla\nabla\cdot\phi}{T_0} = 0 \\ \beta\frac{T_0}{\rho c_E}\nabla\nabla \cdot \mathbf{u} + \frac{T_0}{\rho c_E}\frac{\nabla\nabla\cdot\phi}{T_0} + \omega^2\hat{\rho}\frac{\phi}{T_0} = 0 \end{cases}, \quad (5)$$

where

$$H_{\text{tem}} = H + \frac{\beta^2 T_0}{\rho c_E}, \quad (6)$$

is the longitudinal wave modulus of the background medium, with  $H = \lambda + 2\mu$  being the longitudinal wave modulus. The preceding governing equations are used to describe wave propagation in homogeneous thermoelastic media.

**General solution of the thermoelasticity equations**

The scattered fields for the case of a normally incident P wave impinging on a single circular crack, in a cylindrical coordinate system, can be solved by using the Hankel transform, according to Sherief and El-Maghraby (2003). As these authors, we ignore the macroscopic thermoelastic attenuation in the seismic range. The general solutions of equation 5 for the temperature disturbance, scattered displacements, and stresses can be written as

$$\theta^{\text{sc}}(r, z) = \int_0^\infty \sum_{i=P}^T (k_0^2 - k_i^2) A_i(k) e^{-\eta_i z} J_0(kr) k dk, \quad (7a)$$

$$u_z^{\text{sc}}(r, z) = \int_0^\infty \left[ A_S(k) e^{-\eta_S z} - \frac{\beta}{H} \sum_{i=P}^T A_i(k) \eta_i e^{-\eta_i z} \right] J_0(kr) k dk, \quad (7b)$$

$$u_r^{\text{sc}}(r, z) = \int_0^\infty \left[ A_S(k) \eta_S e^{-\eta_S z} - \frac{\beta}{H} k^2 \sum_{i=P}^T A_i(k) e^{-\eta_i z} \right] J_1(kr) dk, \quad (7c)$$

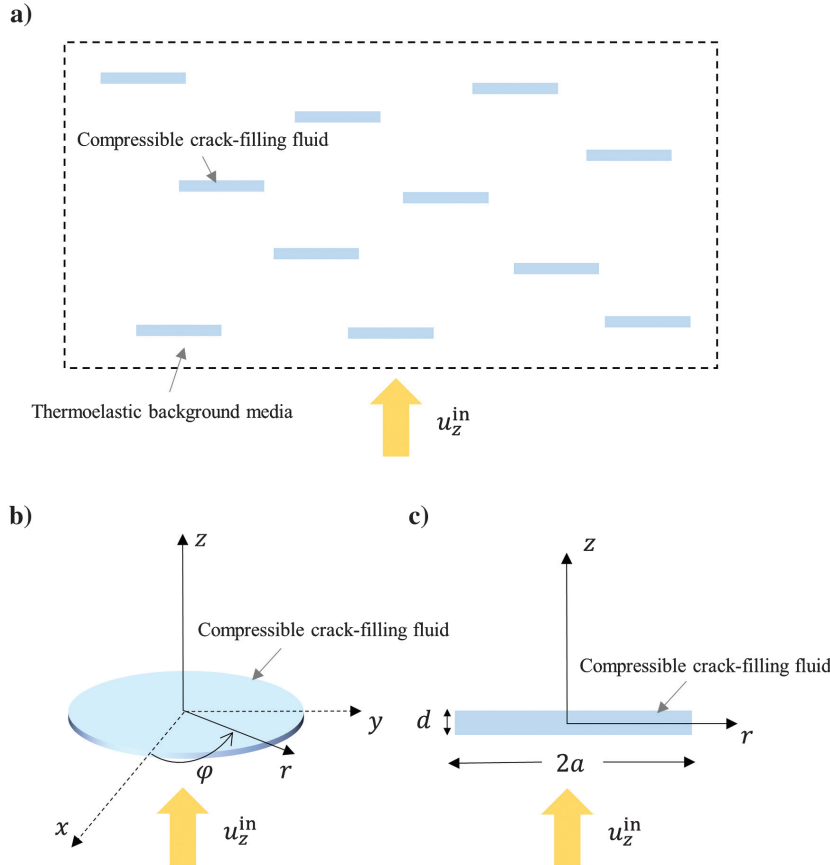


Figure 1. (a) Set of cracks with the same circular shape, sparsely, randomly, and homogeneously embedded in thermoelastic background medium perpendicular to the  $z$ -axis. Each crack has radius  $a$  and thickness  $d$  and is filled with a compressible fluid, as shown in the (b) oblique view and (c) front view. An incident harmonic plane P wave  $u_z^{\text{in}}$  passes through the medium along the axial direction of the cracks.

$$\sigma_{zz}^{sc}(r, z) = \mu \int_0^\infty \left[ \frac{\beta}{H} (2k^2 - k_S^2) \sum_{i=P}^T A_i(k) e^{-\eta_i z} - 2A_S(k) \eta_S e^{-\eta_S z} \right] J_0(kr) k dk, \quad (7d)$$

$$\sigma_{rz}^{sc}(r, z) = \mu \int_0^\infty \left[ \frac{\beta}{H} 2k^2 \sum_{i=P}^T A_i(k) \eta_i e^{-\eta_i z} - (2k^2 - k_S^2) A_S(k) e^{-\eta_S z} \right] J_1(kr) dk, \quad (7e)$$

where the superscript sc denotes the scattered fields; the subscripts P, T, and S denote the thermoelastic P-, T-, and S-wave modes, respectively;  $k_0 = \omega \sqrt{\rho/H}$  is the wavenumber of the P wave in the elastic background;  $k_i$  denotes the wavenumber of the corresponding body wave with  $k_P = \omega \sqrt{\rho/H_{tem}}$ ,  $k_T = \omega \sqrt{\hat{\rho} H_{tem} / (T_0 / \rho c_E) H}$ , and  $k_S = \omega \sqrt{\rho/\mu}$ ;  $\eta_i$  ( $i = P, T, S$ ) are  $\eta_i = k^2 - k_i^2$ ; and  $J_0(kr)$  and  $J_1(kr)$  are the Bessel function of the first kind of order zero and first, respectively. Substituting equation 7a into equation 4 yields the following thermal flux:

$$\phi_z^{sc}(r, z) = -\frac{T_0}{\hat{\rho} \omega^2} \int_0^\infty \sum_{i=P}^T (k_0^2 - k_i^2) A_i(k) \eta_i e^{-\eta_i z} J_0(kr) k dk, \quad (7f)$$

$$\phi_r^{sc}(r, z) = -\frac{T_0}{\hat{\rho} \omega^2} \int_0^\infty \sum_{i=P}^T (k_0^2 - k_i^2) A_i(k) e^{-\eta_i z} J_1(kr) k^2 dk. \quad (7g)$$

Based on the three scalar spectral amplitude functions  $A_i(k)$ , equations 7a–7g provide the general solutions to the scattering problem. To determine the unknown coefficient  $A_i(k)$ , we need the boundary conditions on the plane  $z = 0$ .

### Exact solutions for thermally permeable and impermeable boundary conditions

The normal component of the scattered displacements and thermal flux outside the crack filled with a compressible fluid are zero on the plane  $z = 0$ , and the shear stress is zero. For the permeable case, the thermal flux rapidly diffuses through the crack surface. Thus, the temperature disturbance at the crack boundary is zero (Zhong and Lee, 2012). Combined with equation 1, the boundary conditions in this case are

$$\sigma_{rz}^{sc}(r, 0) = 0, \quad r \geq 0, \quad (8a)$$

$$\sigma_{zz}^{in}(r, 0) + \sigma_{zz}^{sc}(r, 0) = 2K_f \frac{u_z^{sc}(r, 0)}{d}, \quad 0 \leq r \leq a, \quad (8b)$$

$$u_z^{sc}(r, 0) = 0, \quad r > a, \quad (8c)$$

$$\theta^{sc}(r, 0) = 0, \quad 0 \leq r \leq a, \quad (8d)$$

$$\phi_z^{sc}(r, 0) = 0, \quad r > a, \quad (8e)$$

where  $K_f$  is the bulk modulus of the fluid. Substituting the general solutions 7a, 7e, and 7f into the boundary conditions 8a, 8d, and 8e yields

$$A_S(k) = \frac{2\frac{\beta}{H} k^2 [A_P(k) \eta_P + A_T(k) \eta_T]}{2k^2 - k_S^2}, \quad r \geq 0, \quad (9a)$$

$$A_T(k) = -\frac{k_0^2 - k_P^2}{k_0^2 - k_T^2} A_P(k), \quad 0 \leq r \leq a, \quad (9b)$$

$$A_T(k) = -\frac{k_0^2 - k_P^2}{k_0^2 - k_T^2} \frac{\eta_P}{\eta_T} A_P(k), \quad r > a. \quad (9c)$$

We then substitute these relations equations into the general solutions 7b and 7d, and we use the boundary conditions 8b and 8c to obtain a pair of dual integral equations:

$$\begin{cases} \int_0^\infty A_P(k) Z_1(k) k J_0(kr) dk = \frac{ik_P H_{tem} u_0}{\mu \frac{\beta}{H}}, & 0 \leq r \leq a \\ \int_0^\infty \frac{A_P(k) \eta_P}{2k^2 - k_S^2} k J_0(kr) dk = 0, & r > a \end{cases}, \quad (10)$$

where

$$Z_1(k) = \frac{2K_f}{\mu d} \frac{k_S^2}{2k^2 - k_S^2} (\eta_P - \chi \eta_T) - \frac{[(2k^2 - k_S^2)^2 - 4k^2 \eta_S \eta_P] - [(2k^2 - k_S^2)^2 - 4k^2 \eta_S \eta_T] \chi}{2k^2 - k_S^2}, \quad (11)$$

with

$$\chi = \frac{k_0^2 - k_P^2}{k_0^2 - k_T^2}. \quad (12)$$

On the other hand, in the impermeable case, the thermal flux cannot diffuse through the crack surface, so that this flux at the crack boundary is zero (Zhong and Lee, 2012). Wei et al. (2020a) estimate the dispersion and attenuation of P and SV waves in an elastic background containing cracks constrained by this boundary condition. In this case,

$$\sigma_{rz}^{sc}(r, 0) = 0, \quad r \geq 0, \quad (13a)$$

$$\sigma_{zz}^{\text{in}}(r, 0) + \sigma_{zz}^{\text{sc}}(r, 0) = 2 \left( K_f + \frac{\beta_f^2 T_0}{\rho_f c_f} \right) \frac{u_z^{\text{sc}}(r, 0)}{d}, \quad 0 \leq r \leq a, \quad (13b)$$

$$u_z^{\text{sc}}(r, 0) = 0, \quad r > a, \quad (13c)$$

$$\phi_z^{\text{sc}}(r, 0) = 0, \quad r \geq 0, \quad (13d)$$

where  $\beta_f = 3K_f\alpha_f$  with  $\alpha_f$  being the thermal expansion coefficient,  $\rho_f$  is the mass density, and  $c_f$  is the specific heat capacity of the crack-filling fluid. Similarly, a pair of dual integral equation 10 can be obtained, with

$$Z_1(k) = \frac{2 \left( K_f + \frac{\beta_f^2 T_0}{\rho_f c_f} \right) k_S^2}{\mu d} \frac{k_S^2}{2k^2 - k_S^2} (\eta_P - \chi \eta_T) - \frac{[(2k^2 - k_S^2)^2 - 4k^2 \eta_S \eta_P] - [(2k^2 - k_S^2)^2 - 4k^2 \eta_S \eta_T] \chi}{2k^2 - k_S^2} \quad (14)$$

and

$$\chi = \frac{k_0^2 - k_P^2 \eta_P}{k_0^2 - k_T^2 \eta_T}. \quad (15)$$

To obtain the scalar spectral amplitude function  $A_P(k)$  by solving the preceding dual integral equation 10, the following new function is introduced (Noble, 1963):

$$\phi(k) = \frac{c \eta_P k A_P(k)}{2k^2 - k_S^2}, \quad (16)$$

where

$$c = \lim_{k \rightarrow \infty} \frac{Z_1(k)(2k^2 - k_S^2)}{\eta_P k} = -\frac{2(k_P^2 - k_T^2)(k_0^2 - k_S^2)}{k_0^2 - k_T^2}. \quad (17)$$

Then, the pair of dual integral equation 10 can be transformed to

$$\begin{cases} \int_0^\infty Z(k) \phi(k) J_0(kr) k dk = \frac{ik_P H_{\text{tem}} u_0}{\mu \frac{\beta}{H}}, & 0 \leq r \leq a, \\ \int_0^\infty \phi(k) J_0(kr) dk = 0, & r > a \end{cases}, \quad (18)$$

where

$$Z(k) = \frac{2k^2 - k_S^2}{c \eta_P k} Z_1(k). \quad (19)$$

Noble (1963) proves that equation 16 can be expressed as

$$\phi(k) = \int_0^a \psi(r) \sin(kr) dr. \quad (20)$$

After some steps, equation 18 can be converted into a single Fredholm integral equation of the second kind including the unknown function  $\psi(r)$  as

$$\psi(r) - \int_0^a K(s, r) \psi(s) ds = h(r), \quad 0 \leq r \leq a, \quad (21)$$

where the kernel function is

$$K(s, r) = \frac{2}{\pi} \int_0^\infty [1 - Z(k)] \sin(ks) \sin(kr) dk, \quad (22)$$

and the inhomogeneous term is

$$h(r) = \frac{2}{\pi} \int_0^r \frac{k}{\sqrt{r^2 - k^2}} \frac{ik_P H_{\text{tem}} u_0}{\mu \frac{\beta}{H}} dk = \frac{2}{\pi} \frac{ik_P H_{\text{tem}} u_0}{\mu \frac{\beta}{H}} r. \quad (23)$$

The unknown function  $\psi(r)$  can be solved numerically by the quadrature method; then, we can use equation 20 to obtain  $\phi(k)$  and  $A_P(k)$  from equation 16.

### Sparse distribution aligned-crack model

For the purpose of calculating the effective far-field wave phase velocity and attenuation caused by the sparse distribution aligned-crack model, we need to compute the far-field forward scattering amplitude of a single crack:

$$A_P(0) = \frac{k_S^2}{ick_P} \lim_{k \rightarrow 0} \frac{\phi(k)}{k} = \frac{k_S^2}{ick_P} \int_0^a \psi(r) r dr. \quad (24)$$

If cracks are sparse and randomly distributed in the medium, as shown in Figure 1a, multiple scattering can be ignored. We can perform the calculation in the propagation direction based on the Foldy approximation. The far-field forward scattering amplitude  $f(0)$  of a normally incident P wave propagating in a cracked and porous fluid-saturated medium has been derived by Galvin and Gurevich (2009). Based on this work, we obtain

$$f(0) = \frac{\beta}{H} \frac{A_P(0) k_P^2}{u_0}. \quad (25)$$

The effective wavenumbers can be expressed as

$$k_{\text{eff}} = k_P \left[ 1 + \frac{2\pi n_0}{k_P^2} f(0) \right], \quad (26)$$

where  $n_0$  is the number of cracks per unit volume. The phase velocity  $V_P$  and dissipation factor  $Q_P^{-1}$  of the P wave are then (e.g., Carcione, 2014)

$$\begin{cases} V_P = \frac{\omega}{\text{Re}(k_{\text{eff}})} \\ Q_P^{-1} = 2 \frac{\text{Im}(k_{\text{eff}})}{\text{Re}(k_{\text{eff}})} \end{cases}, \quad (27)$$

where  $\text{Re}(k_{\text{eff}})$  and  $\text{Im}(k_{\text{eff}})$  represent the real and imaginary parts of  $k_{\text{eff}}$ , respectively.

### EXAMPLES

The velocity dispersion and attenuation of the normally incident P wave as a function of the dimensionless frequency  $|k_T a|$  are calculated for the permeable and impermeable cases. We consider the following properties of Carcione et al. (2020b):  $K = \lambda + (2\mu/3)$ : 39 GPa,  $G = \mu$ : 39 GPa,  $\rho$ : 2650 kg/m<sup>3</sup>,  $c_V = \rho c_E$ :  $106 \times 10^6$  kg/(m · s<sup>2</sup> · °K),  $\gamma$ : 532 m · kg/(s<sup>3</sup> · °K),  $\beta$ :  $117 \times 10^6$  kg/(m · s<sup>2</sup> · °K), and  $\tau_0 = \gamma/(c_E H)$ :  $1.73 \times 10^{-13}$  s.

The crack has a radius  $a = 10$  m and thickness  $d = 0.1$  m, and the dimensionless crack density is  $\varepsilon = n_0 a^3 = 0.09$ . The fluid properties at 10 MPa are  $T_0 = 373^\circ\text{K}$ ,  $\rho_f = 962.9$  kg/m<sup>3</sup>, and  $c_f = 962.9$  kg/m<sup>3</sup> (Kretzschmar and Wagner, 2019), and we consider two sets of parameters: (1)  $\alpha_f = 260.5 \times 10^{-6} \text{K}^{-1}$  with

$K_f = 1.11, 2.11,$  and  $4.11$  GPa and (2)  $K_f = 2.11$  GPa with  $\alpha_f = 20.5 \times 10^{-6}, 420.5 \times 10^{-6},$  and  $820.5 \times 10^{-6} \text{K}^{-1}$ .

Figure 2 shows the phase velocity (Figure 2a) and dissipation factor (Figure 2b) due to P-wave scattering for the first set of parameters and permeable boundary condition, where we can see two peaks, related to (1) the low-frequency WITF effect and (2) the high-frequency elastic scattering, especially when  $K_f$  value is relatively high. The velocity increases monotonically with frequency, corresponding to the low-frequency peak, and decreases in the Rayleigh scattering regime and increases rapidly in the Mie scattering one, corresponding to the high-frequency peak. In particular, when the thermal wavelength or the elastic wavelength is comparable to the crack size ( $1 < |k_T a| < 10$  or  $1 < |k_p a| < 10$ ), the velocity dispersion is severe, and attenuation has a peak. Due to the interference of the scattered waves from the crack tip, the phase velocity and dissipation factor fluctuate in the high-frequency range (Kawahara and Yamashita, 1992). Figures 3, 4, 5, 6, 7, and 8 show a similar phenomenon. Moreover, we note that the anelasticity is strong

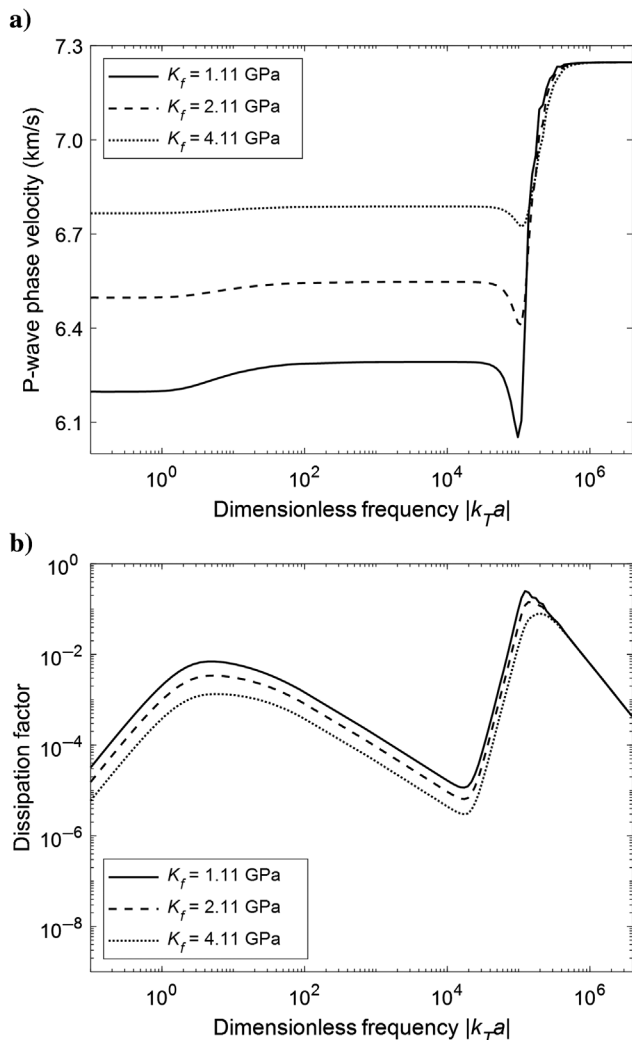


Figure 2. (a) Phase velocity and (b) dissipation factor of P waves as a function of the dimensionless frequency  $|k_T a|$  for the first set of parameters and permeable boundary condition.

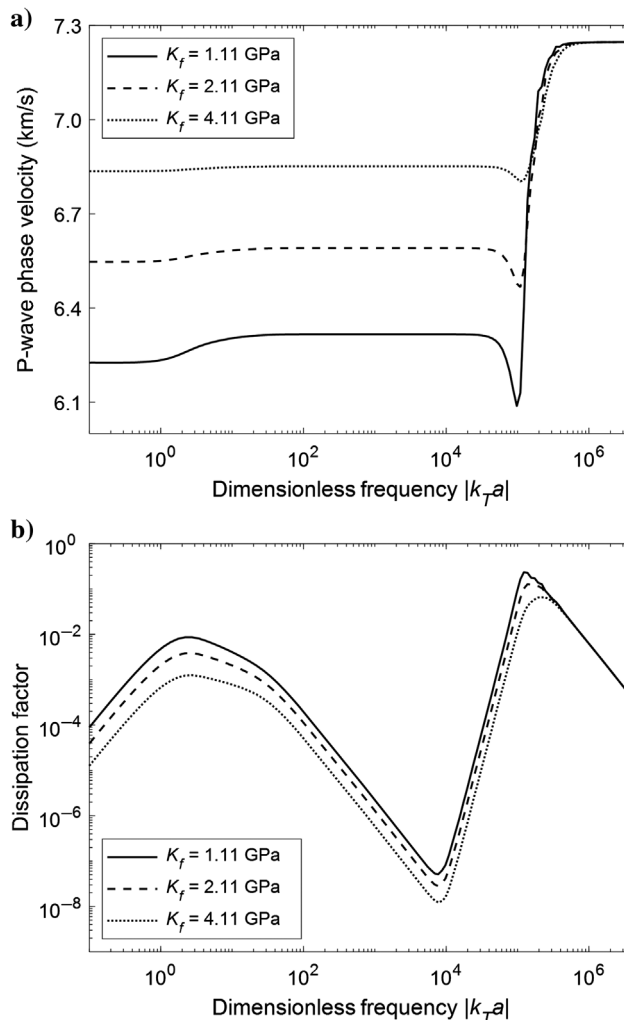


Figure 3. Same as Figure 2, but with impermeable boundary condition.

by decreasing  $K_f$  because cracks are more easily compressed, leading to more temperature variations. The characteristic frequency of the elastic scattering also decreases with decreasing  $K_f$ , but its influence on the WTF characteristic frequency can be ignored. All the curves converge to the same value at the high-frequency limit, which correspond to the P-wave velocity and dissipation factor of the thermoelastic background medium.

Figure 3 depicts the same curves for the impermeable boundary condition. The general trend is similar to that of the permeable case. However, the dissipation is generally weaker, with a relatively small WTF-dominated frequency range due to the much steeper slope of the dispersion and attenuation curves. Moreover, the WTF characteristic frequency moves to lower frequencies.

The phase velocity (Figure 4a) and dissipation factor (Figure 4b) for the second set of parameters, and permeable boundary condition, are shown in Figure 4. We observe that the P-wave dispersion and attenuation do not change with the thermal

expansion coefficient  $\alpha_f$ , which means that this property of the fluid cannot be estimated from the seismic response when the crack surface is fully thermally permeable. Figure 5 displays the impermeable case, showing that the anelasticity increases with decreasing  $\alpha_f$ .

The P-wave phase velocity and dissipation factor are calculated for three different dimensionless crack densities  $\varepsilon = 0.01, 0.03,$  and  $0.09$  with  $\alpha_f = 260.5 \times 10^{-6} \text{K}^{-1}$  and  $K_f = 2.11 \text{ GPa}$  and the two types of boundary conditions (see Figures 6 and 7). In both cases, the anelasticity is stronger for high crack densities, but the characteristic frequencies of the two attenuation mechanisms do not change, with the spatial inhomogeneous scale for inducing WTF smaller than that of elastic scattering.

Finally, Figure 8 compares our results with those of the aligned-circular-cracks elastic-scattering model (Zhang and Gross, 1993) for  $K_f = 2.11 \text{ GPa}$ ,  $\alpha_f = 260.5 \times 10^{-6} \text{K}^{-1}$ , and  $\varepsilon = 0.09$ . In the high-frequency elastic scattering region, the dispersion and at-

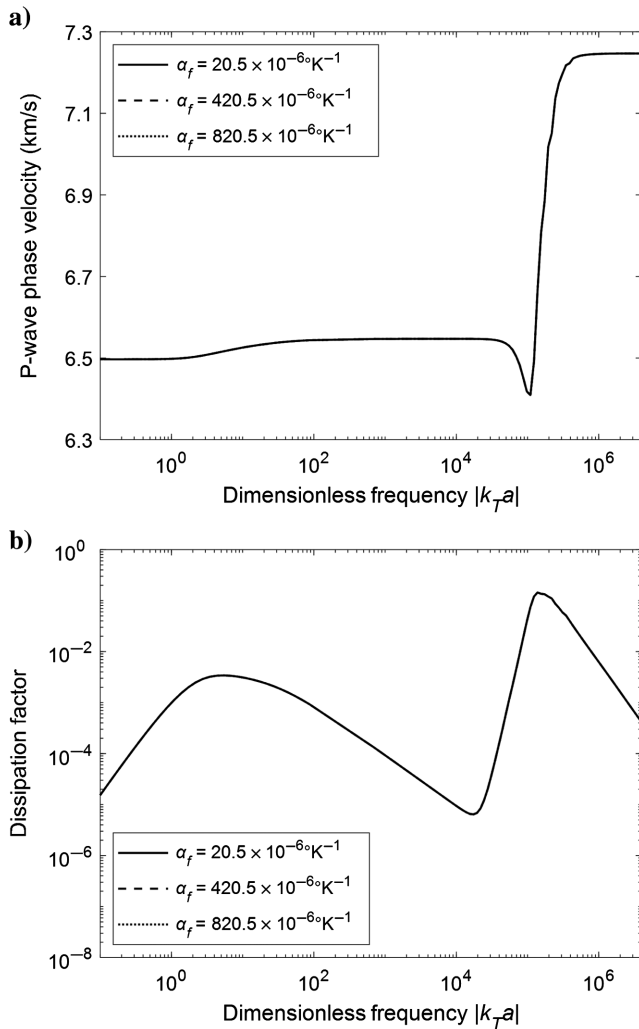


Figure 4. (a) Phase velocity and (b) dissipation factor of P waves as a function of  $|k_T a|$  for the second set of parameters and permeable boundary condition.

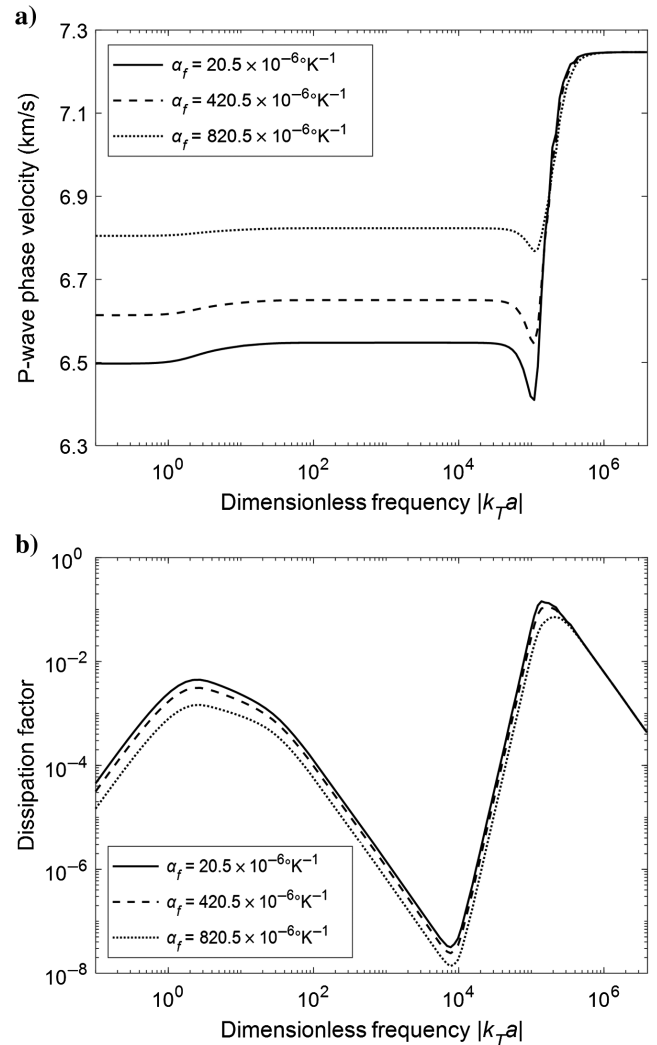


Figure 5. Same as Figure 4, but with impermeable boundary condition.

tenuation curves in the permeable case coincide with those of the preceding scattering model, and the dissipation is stronger than that of the impermeable case (for a detailed explanation, see Wei et al., 2020a). In the low-frequency WITF region, the scattering model has no effect, and the low-frequency limit is the same as that of the impermeable case.

## DISCUSSION

We have analyzed the combined effect of WITF and scattering of P waves from a random distribution of fluid-saturated cracks. The results show that WITF is usually observed at low values of  $|k_T a|$ , whereas scattering is most likely to occur at high  $|k_T a|$ , i.e., high frequencies. Then, these two loss mechanisms can be separated due to their different frequency ranges and phenomenologically modeled with a generalized Zener model to compute synthetic seismograms.

The proposed theory establishes a direct relation between seismic dissipation and the thermoelastic properties of the lithosphere, such as the thermal permeability of the crack interfaces (Figures 2 and 3), which can provide useful information on the earth structure, such as the distribution of the hydrocarbons and sources of geothermal energy (e.g., Kjartansson, 1980). In principle, the theory can be complemented with other models to estimate temperature, partial melting, water content, and rock composition (e.g., Romanowicz and Mitchell, 2007; Carcione et al., 2020a). A limitation is that the approach is only valid for low crack densities. Hence, it is relevant to extend the model to high crack densities (e.g., Benites et al., 1992). Moreover, we consider the dissipation of a normally incident P wave. In this sense, extension to the anisotropic case is required, as well as to consider the effect of WIFF and squirt flow (e.g., Carcione et al., 2018a, 2018b), mostly affected by the fluid viscosity.

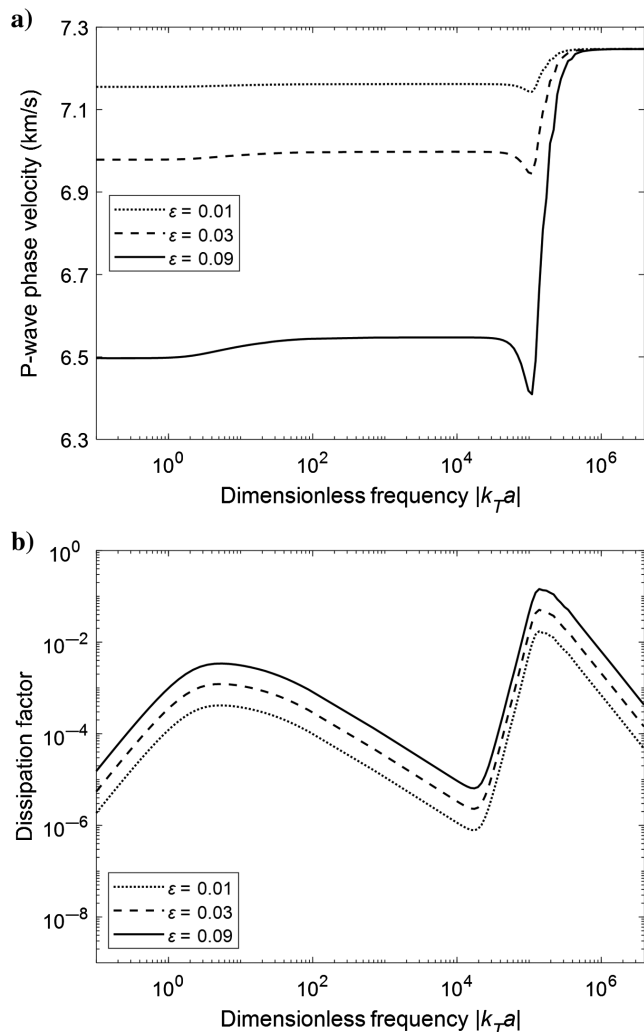


Figure 6. (a) Phase velocity and (b) dissipation factor of P waves as a function of  $|k_T a|$  for three different values of  $\epsilon = n_0 a^3$  and permeable boundary condition.

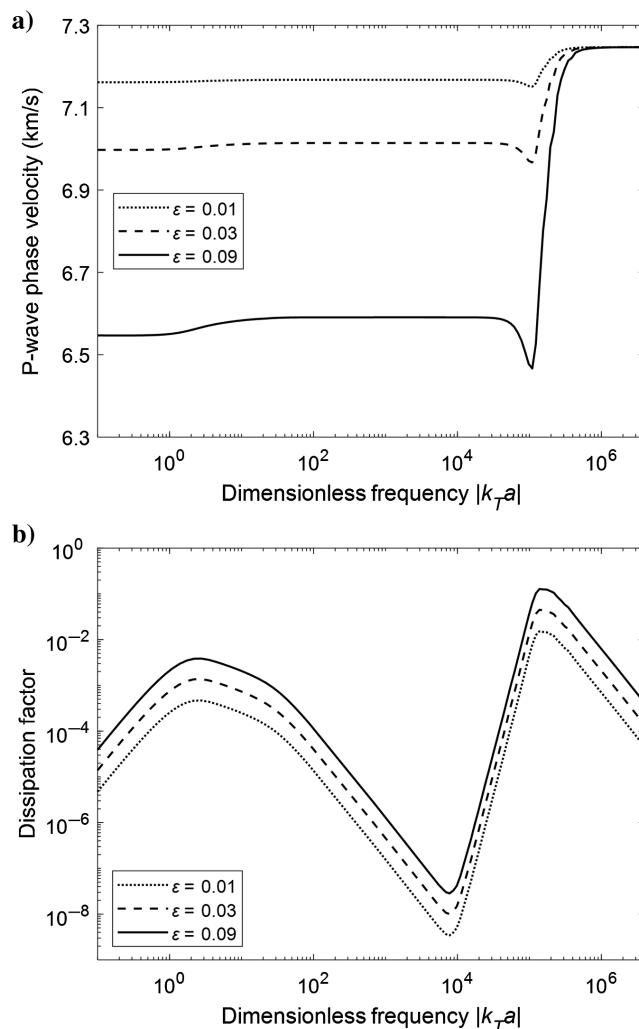


Figure 7. Same as Figure 6, but with impermeable boundary condition.

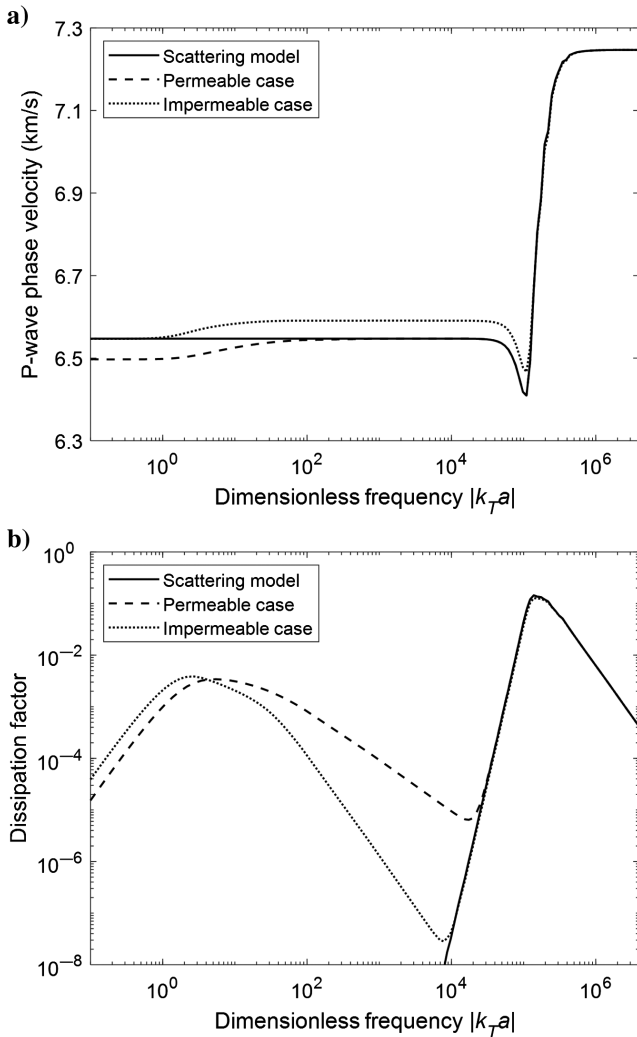


Figure 8. (a) Phase velocity and (b) dissipation factor of P waves as a function of  $|k_T a|$  for the scattering model, and permeable and impermeable cases with  $K_f = 2.11$  GPa,  $\alpha_f = 260.5 \times 10^{-6} \text{K}^{-1}$ , and  $\varepsilon = 0.09$ .

## CONCLUSION

We have developed an effective aligned-crack model to obtain the frequency-dependent phase velocity and attenuation of P waves scattered by a sparse distribution of fluid-saturated cracks in a thermoelastic medium, assuming permeable and impermeable boundary conditions at the crack surface. The examples show that the WITF mechanism and elastic scattering dominate the dissipation at low and high frequencies, respectively. The WITF and scattering attenuation peaks occur when the thermal wavelength or the elastic wavelength is of the same order of the crack size, respectively. Permeable and impermeable crack interfaces display a similar behavior of dispersion and attenuation, which decrease with the crack-filling fluid bulk modulus. The impermeable case (the lack of diffusion of the thermal flux at the crack interface) shows a weaker attenuation and a reduced frequency range of the WITF mechanism. The effect of fluid thermal properties, such as the thermal expansion coefficient, is similar to that of the compressibility in the impermeable case, and it shows no effect in the permeable case. In principle,

it is feasible to estimate the thermoelastic properties and the size of the heterogeneities from seismic attributes, based on the proposed model.

## ACKNOWLEDGMENTS

The research was supported by the National Natural Science Foundation of China (grant no. 41821002), and 111 Project “Deep-Super-deep Oil & Gas Geophysical Exploration” (B18055). No experimental data are used in this paper.

## DATA AND MATERIALS AVAILABILITY

Data associated with this research are available and can be obtained by contacting the corresponding author.

## REFERENCES

- Aki, K., 1980, Attenuation of shear-waves in the lithosphere for frequencies from 0.05 to 25 Hz: *Physics of the Earth and Planetary Interiors*, **21**, 50–60, doi: [10.1016/0031-9201\(80\)90019-9](https://doi.org/10.1016/0031-9201(80)90019-9).
- Armstrong, B. H., 1984, Models for thermoelastic attenuation of waves in heterogeneous solids: *Geophysics*, **49**, 1032–1040, doi: [10.1190/1.1441718](https://doi.org/10.1190/1.1441718).
- Ba, J., W. Xu, L. Fu, J. M. Carcione, and L. Zhang, 2017, Rock anelasticity due to patchy saturation and fabric heterogeneity: A double double-porosity model of wave propagation: *Journal of Geophysical Research: Solid Earth*, **122**, 1949–1976, doi: [10.1002/2016JB013882](https://doi.org/10.1002/2016JB013882).
- Ba, J., J. Zhao, J. M. Carcione, and X. Huang, 2016, Compressional wave dispersion due to rock matrix stiffening by clay squirt flow: *Geophysical Research Letters*, **43**, 6186–6195, doi: [10.1002/2016GL069312](https://doi.org/10.1002/2016GL069312).
- Benites, R., K. Aki, and K. Yomogida, 1992, Multiple scattering of SH waves in 2-D media with many cavities: *Pure and Applied Geophysics*, **138**, 353–390, doi: [10.1007/BF00876878](https://doi.org/10.1007/BF00876878).
- Biot, M. A., 1956, Thermoelasticity and irreversible thermodynamics: *Journal of Applied Physics*, **27**, 240–253, doi: [10.1063/1.1722351](https://doi.org/10.1063/1.1722351).
- Boschi, E., 1973, A thermoviscoelastic model of the earthquake source mechanism: *Journal of Geophysical Research*, **78**, 7733–7737, doi: [10.1029/JB078i032p07733](https://doi.org/10.1029/JB078i032p07733).
- Brajanovski, M., B. Gurevich, and M. Schoenberg, 2005, A model for P-wave attenuation and dispersion in a porous medium permeated by aligned fractures: *Geophysical Journal International*, **163**, 372–384, doi: [10.1111/j.1365-246X.2005.02722.x](https://doi.org/10.1111/j.1365-246X.2005.02722.x).
- Carcione, J. M., 2014, Wave fields in real media. Theory and numerical simulation of wave propagation in anisotropic, anelastic and porous media, 3rd ed.: Elsevier.
- Carcione, J. M., F. Cavallini, E. Wang, J. Ba, and L. Y. Fu, 2019, Physics and simulation of wave propagation in linear thermo-poroelastic media: *Journal of Geophysical Research*, **124**, 8147–8166, doi: [10.1029/2019JB017851](https://doi.org/10.1029/2019JB017851).
- Carcione, J. M., B. Farina, F. Poletto, A. N. Qadrouh, and W. Cheng, 2020a, Seismic attenuation in partially molten rocks: *Physics of the Earth and Planetary Interiors*, **309**, 106568, doi: [10.1016/j.pepi.2020.106568](https://doi.org/10.1016/j.pepi.2020.106568).
- Carcione, J. M., D. Gei, J. E. Santos, L. Y. Fu, and J. Ba, 2020b, Canonical analytical solutions of wave-induced thermoelastic attenuation: *Geophysical Journal International*, **221**, 835–842, doi: [10.1093/gji/ggaa033](https://doi.org/10.1093/gji/ggaa033).
- Carcione, J. M., F. Poletto, and B. Farina, 2018a, The Burgers/squirt-flow seismic model of the crust and mantle: *Physics of the Earth and Planetary Interiors*, **274**, 14–22, doi: [10.1016/j.pepi.2017.10.008](https://doi.org/10.1016/j.pepi.2017.10.008).
- Carcione, J. M., F. Poletto, B. Farina, and C. Bellezza, 2018b, 3D seismic modeling in geothermal reservoirs with a distribution of steam patch sizes, permeabilities and saturations, including ductility of the rock frame: *Physics of the Earth and Planetary Interiors*, **279**, 67–78, doi: [10.1016/j.pepi.2018.03.004](https://doi.org/10.1016/j.pepi.2018.03.004).
- Carcione, J. M., Z. W. Wang, W. Ling, E. Salusti, J. Ba, and L. Y. Fu, 2018c, Simulation of wave propagation in linear thermoelastic media: *Geophysics*, **84**, no. 1, T1–T11, doi: [10.1190/geo2018-0448.1](https://doi.org/10.1190/geo2018-0448.1).
- Chapman, M., 2009, Modeling the effect of multiple sets of mesoscale fractures in porous rock on frequency-dependent anisotropy: *Geophysics*, **74**, no. 6, D97–D103, doi: [10.1190/1.3204779](https://doi.org/10.1190/1.3204779).
- Chapman, M., S. V. Zatsepin, and S. Crampin, 2002, Derivation of a microstructural poroelastic model: *Geophysical Journal International*, **151**, 427–451, doi: [10.1046/j.1365-246X.2002.01769.x](https://doi.org/10.1046/j.1365-246X.2002.01769.x).
- Foldy, L. L., 1945, The multiple scattering of waves. I. General theory of isotropic scattering by randomly distributed scatterers: *Physical Review*, **67**, 107, doi: [10.1103/PhysRev.67.107](https://doi.org/10.1103/PhysRev.67.107).

- Fu, B. Y., L. Y. Fu, J. Guo, R. J. Galvin, and B. Gurevich, 2020, Semi-analytical solution to the problem of frequency dependent anisotropy of porous media with an aligned set of slit cracks: *International Journal of Engineering Science*, **147**, 103209, doi: [10.1016/j.ijengsci.2019.103209](https://doi.org/10.1016/j.ijengsci.2019.103209).
- Fu, B. Y., J. Guo, L. Y. Fu, S. Glubokovskikh, R. J. Galvin, and B. Gurevich, 2018, Seismic dispersion and attenuation in saturated porous rock with aligned slit cracks: *Journal of Geophysical Research: Solid Earth*, **123**, 6890–6910, doi: [10.1029/2018JB015918](https://doi.org/10.1029/2018JB015918).
- Fu, L. Y., 2012, Evaluation of sweet spot and geopressure in Xihu, Sag: Tech Report, CCL2012-SHPS-0018ADM, Key Laboratory of Petroleum Resource Research, Institute of Geology and Geophysics, Chinese Academy of Sciences.
- Fu, L. Y., 2017, Deep-superdeep oil gas geophysical exploration 111: Program report jointly initiated by MOE and SAFEA, B18055, School of Geosciences China University of Petroleum (East China).
- Galvin, R. J., and B. Gurevich, 2009, Effective properties of a poroelastic medium containing a distribution of aligned cracks: *Journal of Geophysical Research: Solid Earth*, **114**, B07305, doi: [10.1029/2008JB006032](https://doi.org/10.1029/2008JB006032).
- Guo, J., J. Germán Rubino, N. D. Barbosa, S. Glubokovskikh, and B. Gurevich, 2018a, Seismic dispersion and attenuation in saturated porous rocks with aligned fractures of finite thickness: Theory and numerical simulations — Part 1: P-wave perpendicular to the crack plane: *Geophysics*, **83**, no. 1, WA49–WA62, doi: [10.1190/geo2017-0065.1](https://doi.org/10.1190/geo2017-0065.1).
- Guo, J., J. Germán Rubino, N. D. Barbosa, S. Glubokovskikh, and B. Gurevich, 2018b, Seismic dispersion and attenuation in saturated porous rocks with aligned fractures of finite thickness: Theory and numerical simulations — Part 2: Frequency-dependent anisotropy: *Geophysics*, **83**, no. 1, WA63–WA71, doi: [10.1190/geo2017-0066.1](https://doi.org/10.1190/geo2017-0066.1).
- Guo, J., and B. Gurevich, 2020, Effects of coupling between wave-induced fluid flow and elastic scattering on P-wave dispersion and attenuation in rocks with aligned fractures: *Journal of Geophysical Research: Solid Earth*, **125**, e2019JB018685, doi: [10.1029/2019JB018685](https://doi.org/10.1029/2019JB018685).
- Guo, J., D. Shuai, J. Wei, P. Ding, and B. Gurevich, 2018c, P-wave dispersion and attenuation due to scattering by aligned fluid saturated fractures with finite thickness: Theory and experiment: *Geophysical Journal International*, **215**, 2114–2133, doi: [10.1093/gji/ggy406](https://doi.org/10.1093/gji/ggy406).
- Gurevich, B., M. Brajanovski, R. J. Galvin, T. M. Müller, and J. Toms-Stewart, 2009, P-wave dispersion and attenuation in fractured and porous reservoirs-poroelasticity approach: *Geophysical Prospecting*, **57**, 225–237, doi: [10.1111/j.1365-2478.2009.00785.x](https://doi.org/10.1111/j.1365-2478.2009.00785.x).
- Harumi, K., 1962, Scattering of plane waves by a cavity ribbon in a solid: *Journal of Applied Physics*, **33**, 3588–3593, doi: [10.1063/1.1702451](https://doi.org/10.1063/1.1702451).
- Hou, W., L. Y. Fu, J. M. Carcione, Z. Wang, and J. Wei, 2021, Simulation of thermoelastic waves based on the Lord–Shulman theory: *Geophysics*, **86**, no. 3, T155–T164, doi: [10.1190/geo2020-0515.1](https://doi.org/10.1190/geo2020-0515.1).
- Jacquey, A. B., M. Cacace, G. Blöcher, and M. Scheck-Wenderoth, 2015, Numerical investigation of thermoelastic effects on fault slip tendency during injection and production of geothermal fluids: *Energy Procedia*, **76**, 311–320, doi: [10.1016/j.egypro.2015.07.868](https://doi.org/10.1016/j.egypro.2015.07.868).
- Kawahara, J., and T. Yamashita, 1992, Scattering of elastic waves by a fracture zone containing randomly distributed cracks: *Pure and Applied Geophysics*, **139**, 121–144, doi: [10.1007/BF00876828](https://doi.org/10.1007/BF00876828).
- Kikuchi, M., 1981, Dispersion and attenuation of elastic waves due to multiple scattering from cracks: *Physics of the Earth and Planetary Interiors*, **27**, 100–105, doi: [10.1016/0031-9201\(81\)90037-6](https://doi.org/10.1016/0031-9201(81)90037-6).
- Kjartansson, E., 1980, Attenuation of seismic waves in rocks and applications in energy exploration: Ph.D. thesis, Stanford University.
- Kretzschmar, H. J., and W. Wagner, 2019, *International steam tables: Properties of water and steam based on the industrial formulation IAPWS-IF97*: Springer.
- Lord, H. W., and Y. Shulman, 1967, A generalized dynamical theory of thermoelasticity: *Journal of the Mechanics and Physics of Solids*, **15**, 299–309, doi: [10.1016/0022-5096\(67\)90024-5](https://doi.org/10.1016/0022-5096(67)90024-5).
- Martin, P. A., 1981, Diffraction of elastic waves by a penny-shaped crack: *Proceedings of the Royal Society of London. A. Mathematical and Physical Sciences*, **378**, 263–285, doi: [10.1098/rspa.1981.0151](https://doi.org/10.1098/rspa.1981.0151).
- Müller, T. M., B. Gurevich, and M. Lebedev, 2010, Seismic wave attenuation and dispersion resulting from wave-induced flow in porous rocks — A review: *Geophysics*, **75**, no. 5, 75A147–75A164, doi: [10.1190/1.3463417](https://doi.org/10.1190/1.3463417).
- Noble, B., 1963, The solution of Bessel function dual integral equations by a multiplying-factor method: *Mathematical Proceedings of the Cambridge Philosophical Society*, **59**, 351–362, doi: [10.1017/S0305004100036987](https://doi.org/10.1017/S0305004100036987).
- Parmentier, E. M., and W. F. Haxby, 1986, Thermal stresses in the oceanic lithosphere: Evidence from geoid anomalies at fracture zones: *Journal of Geophysical Research: Solid Earth*, **91**, 7193–7204, doi: [10.1029/JB091iB07p07193](https://doi.org/10.1029/JB091iB07p07193).
- Ritsema, J., A. A. Deuss, H. J. van Heijst, and J. H. Woodhouse, 2011, S40RTS: A degree-40 shear-velocity model for the mantle from new Rayleigh wave dispersion, teleseismic traveltime and normal-mode splitting function measurements: *Geophysical Journal International*, **184**, 1223–1236, doi: [10.1111/j.1365-246X.2010.04884.x](https://doi.org/10.1111/j.1365-246X.2010.04884.x).
- Romanowicz, B., and B. Mitchell, 2007, Deep earth structure: *Q* of the earth from the crust to core: *Treatise on Geophysics*, **1**, 731–774, doi: [10.1016/B978-04452748-6.00024-9](https://doi.org/10.1016/B978-04452748-6.00024-9).
- Sato, H., 2021, SH wavelet propagation through the random distribution of aligned line cracks based on the radiative transfer theory: *Pure and Applied Geophysics*, **178**, 1047–1061, doi: [10.1007/s00024-021-02680-8](https://doi.org/10.1007/s00024-021-02680-8).
- Savage, J., 1966, Thermoelastic attenuation of elastic waves by cracks: *Journal of Geophysical Research*, **71**, 3929–3938, doi: [10.1029/JZ071i016p03929](https://doi.org/10.1029/JZ071i016p03929).
- Sezawa, K., 1927, Scattering of elastic waves and some allied problems: *Bulletin of the Earthquake Research Institute, Tokyo Imperial University*, **3**, 19–41.
- Sherief, H. H., and N. M. El-Maghraby, 2003, An internal penny-shaped crack in an infinite thermoelastic solid: *Journal of Thermal Stresses*, **26**, 333–352, doi: [10.1080/713855898](https://doi.org/10.1080/713855898).
- Shuai, D., A. Stovas, J. Wei, and B. Di, 2020, Frequency-dependent anisotropy due to two orthogonal sets of mesoscale fractures in porous media: *Geophysical Journal International*, **221**, 1450–1467, doi: [10.1093/gji/ggaa081](https://doi.org/10.1093/gji/ggaa081).
- Shuai, D., A. Stovas, Y. Zhao, X. Huang, and L. He, 2022, Frequency-dependent anisotropy due to non-orthogonal sets of mesoscale fractures in porous media: *Geophysical Journal International*, **228**, 102–118, doi: [10.1093/gji/ggab341](https://doi.org/10.1093/gji/ggab341).
- Song, Y., H. Hu, and B. Han, 2020, Effective properties of a porous medium with aligned cracks containing compressible fluid: *Geophysical Journal International*, **221**, 60–76, doi: [10.1093/gji/ggz576](https://doi.org/10.1093/gji/ggz576).
- Song, Y., H. Hu, and J. W. Rudnicki, 2016a, Shear properties of heterogeneous fluid-filled porous media with spherical inclusions: *International Journal of Solids and Structures*, **83**, 154–168, doi: [10.1016/j.ijsolstr.2016.01.009](https://doi.org/10.1016/j.ijsolstr.2016.01.009).
- Song, Y., H. Hu, J. W. Rudnicki, and Y. Duan, 2016b, Dynamic transverse shear modulus for a heterogeneous fluid-filled porous solid containing cylindrical inclusions: *Geophysical Journal International*, **206**, 1677–1694, doi: [10.1093/gji/ggw245](https://doi.org/10.1093/gji/ggw245).
- Treitel, S., 1959, On the attenuation of small-amplitude plane stress waves in a thermoelastic solid: *Journal of Geophysical Research*, **64**, 661–665, doi: [10.1029/JZ064i006p00661](https://doi.org/10.1029/JZ064i006p00661).
- Wang, Z. W., L. Y. Fu, J. Wei, W. Hou, J. Ba, and J. M. Carcione, 2020, On the Green function of the Lord–Shulman thermoelasticity equations: *Geophysical Journal International*, **220**, 393–403, doi: [10.1093/gji/ggz453](https://doi.org/10.1093/gji/ggz453).
- Wei, J., L. Y. Fu, T. Han, and J. M. Carcione, 2020a, Thermoelastic dispersion and attenuation of P and SV wave scattering by aligned fluid-saturated cracks of finite thickness in an isothermal elastic medium: *Journal of Geophysical Research: Solid Earth*, **125**, e2020JB019942, doi: [10.1029/2020JB019942](https://doi.org/10.1029/2020JB019942).
- Wei, J., L. Y. Fu, Z. W. Wang, J. Ba, and J. M. Carcione, 2020b, Green function of the Lord–Shulman thermo-poroelasticity theory: *Geophysical Journal International*, **221**, 1765–1776, doi: [10.1093/gji/ggaa100](https://doi.org/10.1093/gji/ggaa100).
- Yamashita, T., 1990, Attenuation and dispersion of SH waves due to scattering by randomly distributed cracks: *Pure and Applied Geophysics*, **132**, 545–568, doi: [10.1007/BF00876929](https://doi.org/10.1007/BF00876929).
- Zener, C., 1938, Internal friction in solids II. General theory of thermoelastic internal friction: *Physical Review*, **53**, 90, doi: [10.1103/PhysRev.53.90](https://doi.org/10.1103/PhysRev.53.90).
- Zhang, C. H., and D. Gross, 1993, Wave attenuation and dispersion in randomly cracked solids — II. Penny-shaped cracks: *International Journal of Engineering Science*, **31**, 859–872, doi: [10.1016/0020-7225\(93\)90098-F](https://doi.org/10.1016/0020-7225(93)90098-F).
- Zhong, X. C., and K. Y. Lee, 2012, A thermal-medium crack model: *Mechanics of Materials*, **51**, 110–117, doi: [10.1016/j.mechmat.2012.04.013](https://doi.org/10.1016/j.mechmat.2012.04.013).

Biographies and photographs of the authors are not available.